

Visual Attention Network

Meng-Hao Guo¹, Cheng-Ze Lu², Zheng-Ning Liu¹,
Ming-Ming Cheng², and Shi-Min Hu¹

¹ BNRist, Department of Computer Science and Technology, Tsinghua University.

² TKLNDST, College of Computer Science, Nankai University.

gmh20@mails.tsinghua.edu.cn, czlu919@outlook.com, lzhengning@gmail.com,
cmm@nankai.edu.cn, shimin@tsinghua.edu.cn

Abstract. While originally designed for natural language processing (NLP) tasks, the self-attention mechanism has recently taken various computer vision areas by storm. However, the 2D nature of images brings three challenges for applying self-attention in computer vision. (1) Treating images as 1D sequences neglects their 2D structures. (2) The quadratic complexity is too expensive for high-resolution images. (3) It only captures spatial adaptability but ignores channel adaptability. In this paper, we propose a novel large kernel attention (LKA) module to enable self-adaptive and long-range correlations in self-attention while avoiding the above issues. We further introduce a novel neural network based on LKA, namely Visual Attention Network (VAN). While extremely simple and efficient, VAN outperforms the state-of-the-art vision transformers and convolutional neural networks with a large margin in extensive experiments, including image classification, object detection, semantic segmentation, instance segmentation, *etc.* Code is available at <https://github.com/Visual-Attention-Network>.

Keywords: Attention, Vision Backbone, Deep Learning, ConvNets

1 Introduction

As the basic feature extractor, vision backbone is a fundamental research topic in the computer vision field. Due to remarkable feature extraction performance, convolutional neural networks (CNNs) [41,40,39] are indispensable topic in the last decade. After the AlexNet [39] reopened the deep learning decade, a number of breakthroughs have been made to get more powerful vision backbones, by using deeper network [68,29], more efficient architecture [31,90,102], stronger multi-scale ability [35,71,19], and attention mechanisms [34,17]. Due to translation invariance property and shared sliding-window strategy [67], CNNs are inherently efficient for various vision tasks with arbitrary sized input. More advanced vision backbone networks often results in significant performance gain in various tasks, including image classification [29,17,52], object detection [14], semantic segmentation [89] and pose estimation [80].

Based on observed reaction times and estimated signal transmission times along biological pathways [21], cognitive psychology [76] and neuroscience [85]

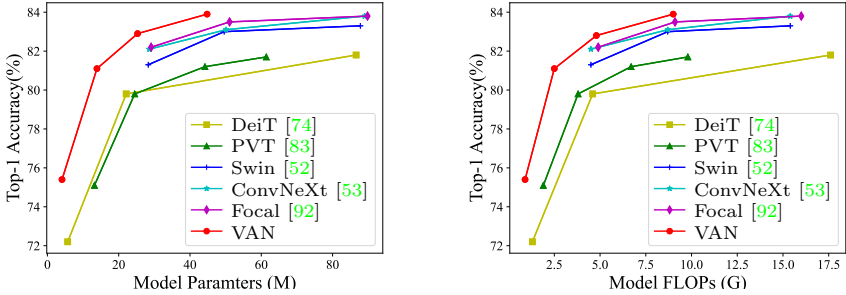


Fig. 1. Results of different models on ImageNet-1K validation set. Left: Comparing the performance of recent models DeiT [74], PVT [83], Swin Transformer [52], ConvNeXt [53], Focal Transformer [92] and our VAN. All these models have a similar amount of parameters. Right: Comparing the performance of recent models and our VAN while keeping the computational cost similar.

, researchers believe that human vision system processes only parts of possible stimuli in detail, while leaving the rest nearly unprocessed. Selective attention is an important mechanism for dealing with the combinatorial aspects of complex search in vision [77]. Attention mechanism can be regarded as an adaptive selecting process based on the input feature. Since the fully attention network [78] been proposed, self-attention models (*a.k.a.*, Transformer) quickly becomes the dominated architecture [16,5] in natural language processing (NLP). Recently, Dosovitskiy *et al.* [17] propose the vision transformer (ViT), which introduces transformer backbone into computer vision and outperforms well-known CNNs on image classification tasks. Benefited from its powerful modeling capabilities, transformer-based vision backbones quickly occupy the leaderboards of various tasks, including object detection [52], semantic segmentation [89], *etc.*

Even with remarkable success, convolution operation and self-attention still have their shortcomings. Convolution operation adopts static weight and lacks adaptability, which has been proven critical [34,14]. As originally designed for 1D NLP tasks, self-attention [17,17] regards 2D images as 1D sequences, which destroys the crucial 2D structure of the image. It is also difficult to process high-resolution images due to its quadratic computational and memory overhead. Besides, self-attention is a special attention that only considers the adaptability in spatial dimension but ignores the adaptability in channel dimension, which is also important for visual tasks [34,86,81,1].

In this paper, we propose a novel attention mechanism dubbed large kernel attention (LKA), which is tailored for visual tasks. LKA absorbs the advantages of convolution and self-attention, including local structure information, long-range dependence and adaptability. Meanwhile, it avoids their disadvantages such as ignoring adaptability in channel dimension. Based on the LKA, we present a novel vision backbone called Visual Attention Network (VAN) that

significantly surpasses well-known CNN-based and transformer-based backbones. The contributions of this paper are summarized as follows:

- We design a novel attention mechanism named LKA for computer vision, which considers the pros of both convolution and self-attention, while avoiding their cons. Based on LKA, we further introduce a simple vision backbone called VAN.
- We show that VANs outperform the state-of-the-art ViTs and CNNs with a large margin in extensive experiments, including image classification, object detection, semantic segmentation, instance segmentation, *etc.*

2 Related Work

2.1 Convolutional Neural Networks

How to effectively compute powerful feature representations is the most fundamental problem in computer vision. The convolutional neural networks (CNNs) [41,40], utilize local contextual information and translation invariance properties to greatly improve the efficiency of neural networks. CNNs quickly become the main mainstream framework in computer vision since AlexNet [39]. To further improve the efficiency, researchers put lots of effort in making the CNNs deeper [68,29,35,71], and lighter [31,65,102]. Our work has similarity with MobileNet [31], which decouples a standard convolution into two parts, a depthwise convolution and a pointwise convolution (*a.k.a.*, 1×1 Conv [43]). Our method decomposes a convolution into three parts: depthwise convolution, depthwise and dilated convolution [9,93], and pointwise convolution. Benefiting from this decomposition, our method is more suitable for efficiently decomposing large kernel convolutions. We also introduce attention mechanism into our method to obtain adaptive property.

2.2 Visual Attention Methods

Attention mechanism can be regarded as an adaptive selection process according to the input feature, which is introduced into computer vision in RAM [56]. It has provided benefits in many visual tasks, such as image classification [34,86], object detection [14,32] and semantic segmentation [96,20]. Attention in computer vision can be divided into four basic categories [25], including channel attention, spatial attention, temporal attention and branch attention, and their combinations such as channel & spatial attention. Each kind of attention has a different effect in visual tasks.

Originating from NLP [78,16], self-attention is a special kind of attention mechanism. Due to its effectiveness of capturing the long range dependence and adaptability, it is playing an increasingly important role in computer vision [84,18,62,97,99,91]. Various deep self-attention networks (*a.k.a.*, vision transformers) [17,7,52,22,69,83,95,47,48,4,50,87,51,27] have achieved significantly better performance than the mainstream CNNs on different visual tasks, showing

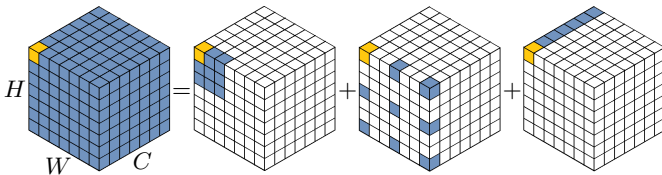


Fig. 2. Decomposition diagram of large-kernel convolution. A standard convolution can be decomposed into three parts: a depth-wise convolution (DW-Conv), a depth-wise dilation convolution (DW-D-Conv) and a 1×1 convolution (1×1 Conv). The colored grids represent the location of convolution kernel and the yellow grid means the center point. The diagram shows that a 13×13 convolution is decomposed into a 5×5 depth-wise convolution, a 5×5 depth-wise dilation convolution with dilation rate 3 and 1×1 convolution. Note: zero paddings are omitted in above figure.

the huge potential of attention-based models. However, self-attention is originally designed for NLP. It has three shortcomings when dealing with computer vision tasks. (1) It treats images as 1D sequences which neglects the 2D structure of images. (2) The quadratic complexity is too expensive for high-resolution images. (3) It only achieves spatial adaptability but ignores the adaptability in channels dimension. For vision tasks, different channels often represent different objects [11,25]. Channel adaptability is also proven important for visual tasks [34,86,60,81,11]. To solve these problems, we propose a novel visual attention method, namely, LKA. It involves the pros of self-attention such as adaptability and long range dependence. Besides, it benefits from the advantages of convolution such as making use of local contextual information.

2.3 Vision MLPs

Multilayer Perceptrons (MLPs) [63,64] were a popular tool for computer vision before CNNs appearing. However, due to high computational requirements and low efficiency, the capability of MLPs was been limited in a long time. Some recent research successfully decouple standard MLP into spatial MLP and channel MLP [72,23,73,46]. Such decomposition allows significant computational cost and parameters reduction, which release the amazing performance of MLP. Readers are referred to recent surveys [24,49] for a more comprehensive review of MLPs. The most related MLP to our is the gMLP [46], which not only decomposes the standard MLP but also involves the attention mechanism. However, gMLP has two drawbacks. On the one hand, gMLP is sensitive to input size and can only process fixed-size images. On the other hand, gMLP only considers the global information of the image and ignore their local structure. Our method can make full use of its advantages and avoid its shortcomings.

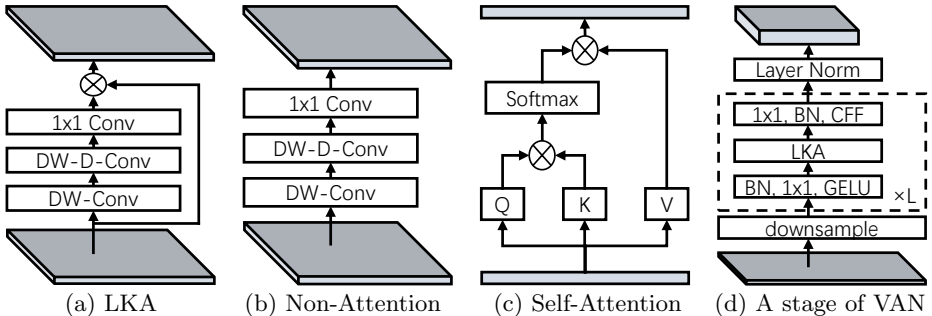


Fig. 3. The structure of different modules: (a) the proposed Large Kernel Attention (LKA); (b) non-attention module; (c) the self-attention module [78]; (d) a stage of our Visual Attention Network (VAN). CFF means convolutional feed-forward network. The difference between (a) and (b) is the element-wise multiply. It is worth noting that (c) is designed for 1D sequences.

3 Method

3.1 Large Kernel Attention

Attention mechanism can be regarded as an adaptive selection process, which can select the discriminative features and automatically ignore noisy responses according to the input features. The key step of attention mechanism is producing attention map which indicates the importance of different points. To do so, we should learn the relationship between different points.

There are two well-known methods to build relationship between different points. The first one is adopting self-attention mechanism [84,97,99,17] to capture long-range dependence. There are three obvious shortcomings for self-attention applied in computer vision which have been listed in Sec. 2.2. The second one is to use large kernel convolution [86,79,33,58] to build relevance and produce attention map. There are still obvious cons in this way. Large-kernel convolution brings a huge amount of computational overhead and parameters.

To overcome above listed cons and make use of the pros of self-attention and large kernel convolution, we propose to decompose a large kernel convolution operation to capture long-range relationship. As shown in Fig. 2, a large kernel convolution can be divided into three components: a spatial local convolution (depth-wise convolution), a spatial long-range convolution (depth-wise dilation convolution) and a channel convolution (1×1 convolution). Specifically, we can decompose a $K \times K$ convolution into a $\frac{K}{d} \times \frac{K}{d}$ depth-wise dilation convolution with dilation d , a $(2d-1) \times (2d-1)$ depth-wise convolution and a 1×1 convolution. Through the above decomposition, we can capture long-range relationship with slight computational cost and parameters. After obtaining long-range relationship, we can estimate the importance of a point and generate attention map.

Table 1. Desirable properties belonging to convolution, self-attention and LKA.

| Properties | Convolution | Self-Attention | LKA |
|-----------------------|-------------|----------------|-----|
| Local Receptive Field | ✓ | ✗ | ✓ |
| Long range dependence | ✗ | ✓ | ✓ |
| Spatial Adaptability | ✗ | ✓ | ✓ |
| Channel Adaptability | ✗ | ✗ | ✓ |

As demonstrated in Fig. 3(a), the LKA module can be written as

$$Attention = Conv_{1 \times 1}(DW-D-Conv(DW-Conv(F))), \quad (1)$$

$$Output = Attention \otimes F. \quad (2)$$

Here, $F \in R^{C \times H \times W}$ is the input feature. $Attention \in R^{C \times H \times W}$ denotes attention map. The value in attention map indicates the importance of each feature. \otimes means element-wise product. As shown in Tab. 1, our proposed LKA combines the advantages of convolution and self-attention. It takes the local contextual information, large receptive field, and dynamic process into consideration. Furthermore, LKA not only achieves the adaptability in the spatial dimension but also the adaptability in the channel dimension. It worth noting that different channels often represent different objects in deep neural networks [25,11] and adaptability in the channel dimension is also important for visual tasks.

3.2 Visual Attention Network (VAN)

Our VAN has a simple hierarchical structure, *i.e.*, a sequence of four stages with decreasing output spatial resolution, *i.e.*, $\frac{H}{4} \times \frac{W}{4}$, $\frac{H}{8} \times \frac{W}{8}$, $\frac{H}{16} \times \frac{W}{16}$ and $\frac{H}{32} \times \frac{W}{32}$ respectively. Here, H and W donate the height and width of the input image. With the decreasing of resolution, the number of output channels is increasing. The change of output channel C_i is presented in Tab. 2.

For each stage as shown in Fig. 3 (d), we firstly downsample the input and use the stride number to control the downsample rate. After the downsample, all other layers in a stage stay the same output size, *i.e.*, spatial resolution and

Table 2. The detailed setting for different versions of the VAN. e.r. represents expansion ratio in the feed-forward network.

| stage | output size | e.r. | VAN-T | VAN-S | VAN-B | VAN-L |
|----------------|---|------|------------------|------------------|-------------------|-------------------|
| 1 | $\frac{H}{4} \times \frac{W}{4} \times C$ | 8 | $C = 32, L = 3$ | $C = 64, L = 2$ | $C = 64, L = 3$ | $C = 64, L = 3$ |
| 2 | $\frac{H}{8} \times \frac{W}{8} \times C$ | 8 | $C = 64, L = 3$ | $C = 128, L = 2$ | $C = 128, L = 3$ | $C = 128, L = 5$ |
| 3 | $\frac{H}{16} \times \frac{W}{16} \times C$ | 4 | $C = 160, L = 5$ | $C = 320, L = 4$ | $C = 320, L = 12$ | $C = 320, L = 27$ |
| 4 | $\frac{H}{32} \times \frac{W}{32} \times C$ | 4 | $C = 256, L = 2$ | $C = 512, L = 2$ | $C = 512, L = 3$ | $C = 512, L = 3$ |
| Parameters (M) | | | 4.1 | 13.9 | 26.6 | 44.8 |
| FLOPs (G) | | | 0.9 | 2.5 | 5.0 | 9.0 |

Table 3. Comparison of parameters of different manners for a 21×21 convolution. X, Y and Our donate standard convolution, mobilenet decomposition [31] and our decomposition respectively. The input and output feature have the same size $H \times W \times C$. Note: Bias is omitted for simplifying format.

| | #Params of X | #Params of Y | #Params of Our | X / Our | Y / Our |
|-------|--------------|--------------|----------------|---------|---------|
| C=32 | 451,584 | 15,136 | 3,392 | 133.13 | 4.46 |
| C=64 | 1,806,336 | 32,320 | 8,832 | 204.52 | 3.66 |
| C=128 | 7,225,344 | 72,832 | 25,856 | 279.45 | 2.82 |
| C=256 | 28,901,376 | 178,432 | 84,480 | 342.11 | 2.11 |
| C=512 | 115,605,504 | 487,936 | 300,032 | 385.31 | 1.63 |

the number of channels. Then, L groups of batch normalization [36], GELU activation [30], large kernel attention and convolutional feed-forward network [82] are stacked in sequence to extract features. Finally, we apply a layer normalization [2] at the end of each stage. We design four architectures VAN-Tiny, VAN-Small, VAN-Base and VAN-Large, according to the parameters and computational cost. The details of the whole network are shown in Tab. 2.

Complexity analysis. We present the parameters and floating point operations (FLOPs) of our decomposition. Bias is omitted in the computation process for simplifying format. We assume that the input and output features have same size $H \times W \times C$. The parameters and FLOPs can be donated as:

$$\mathbf{Params} = \frac{K}{d} \times \frac{K}{d} \times C + (2d - 1) \times (2d - 1) \times C + C \times C, \quad (3)$$

$$\mathbf{FLOPs} = \left(\frac{K}{d} \times \frac{K}{d} \times C + (2d - 1) \times (2d - 1) \times C + C \times C \right) \times H \times W. \quad (4)$$

Here, d means dilation rate and K is kernel size. When $K = 21$, the (3) can be written as:

$$\mathbf{Params} = \left(\frac{21}{d} \times \frac{21}{d} + (2d - 1) \times (2d - 1) \right) \times C + C \times C, d \in Z^+. \quad (5)$$

We find that when $d = 3$, the formula (5) takes the minimum value. So, we set $K = 21$ and $d = 3$ by default. For different number of channels, we show the specific parameters in Tab. 3. According to the formula of FLOPs and parameters, X/Our is same for FLOPs and parameters. Similarly, Y/Our is same for FLOPs and parameters. It indicates that our decomposition owns significant advantages in decomposing large kernel convolution in terms of parameters and FLOPs.

Implementation details. By default, our LKA adopts a 5×5 depth-wise convolution, a 7×7 depth-wise convolution with dilation 3 and a 1×1 convolution to approximate a 21×21 convolution. Under this setting, VAN can effectively achieve both local information as well as long-range connections. We use 7×7 and 3×3 stride convolutions for $4 \times$ and $2 \times$ downsampling respectively.

Table 4. Ablation study of different modules in LKA. Results show that each part is critical. Acc(%) means Top-1 accuracy on ImageNet validation set. ✓ in the attention column we use the Figure 3(a) structure. ✗ in attention column we use the Figure 3(b) structure.

| Method | DW-Conv | DW-D-Conv | Attention | 1×1 Conv | Acc(%) |
|----------|---------|-----------|-----------|-------------------|--------|
| VAN-Tiny | ✗ | ✓ | ✓ | ✓ | 74.9 |
| VAN-Tiny | ✓ | ✗ | ✓ | ✓ | 74.1 |
| VAN-Tiny | ✓ | ✓ | ✗ | ✓ | 74.3 |
| VAN-Tiny | ✓ | ✓ | ✓ | ✗ | 74.6 |
| VAN-Tiny | ✓ | ✓ | ✓ | ✓ | 75.4 |

4 Experiments

In this section, quantitative and qualitative experiments are exhibit to demonstrate the effectiveness of the proposed VAN. We conduct quantitative experiments on ImageNet-1K [15] image classification dataset, COCO [45] object detection dataset and ADE20K [105] semantic segmentation dataset. Furthermore, we visualize the class activation mapping(CAM) [104] by using Grad-CAM [66] on ImageNet validation set. All models are trained with 8 RTX 3090 or A100 GPUs.

4.1 Image Classification

Settings. We conduct image classification on ImageNet-1K [15] dataset. It contains 1.28M training images and 50K validation images from 1,000 different categories. The whole training scheme mostly follows [74]. We adopt random clipping, random horizontal flipping, label-smoothing [57], mixup [100], cut-mix [98] and random erasing [103] to augment the training data. In the training process, we train our VAN for 310 epochs by using AdamW [37,55] optimizer with momentum=0.9, weight decay= 5×10^{-2} and batch size = 1,024. Cosine schedule [54] and warm-up strategy are employed to adjust the learning rate(LR). The initial LR is set to 5×10^{-4} . We adopt a variant of LayerScale [75] which replaces $x_{out} = x + \text{diag}(\lambda_1, \lambda_2, \dots, \lambda_d)f(x)$ with $x_{out} = x + \text{diag}(\lambda_1, \lambda_2, \dots, \lambda_d)(f(x) + x)$ with initial value 0.01 and achieves a better performance than original LayerScale. Exponential moving average (EMA) [59] is also applied to improve training process. During the eval stage, we report the top-1 accuracy on ImageNet validation set under single crop setting.

Ablation Study. We conduct an ablation study to prove that each component of LKA is critical. In order to obtain experimental results quickly, we choose VAN-Tiny as our baseline model. The experimental results in the Tab. 4 indicate that all components in LKA are indispensable to improve performance.

- **DW-Conv.** DW-Conv can make use of the local contextual information of images. Without it, the classification performance will drop by 0.5% (74.9%

Table 5. Compare with the state-of-the-art methods on ImageNet validation set. Params means parameter. GFLOPs donates floating point operations. Top-1 Acc represents Top-1 accuracy.

| Method | Params. (M) | GFLOPs | Top-1 Acc (%) |
|-------------------------------|-------------|--------|---------------|
| PVTv2-B0 [82] | 3.4 | 0.6 | 70.5 |
| T2T-ViT-7 [95] | 4.3 | 1.1 | 71.7 |
| DeiT-Tiny/16 [74] | 5.7 | 1.3 | 72.2 |
| TNT-Ti [26] | 6.1 | 1.4 | 73.9 |
| VAN-Tiny(Our) | 4.1 | 0.9 | 75.4 |
| ResNet18 [29] | 11.7 | 1.8 | 69.8 |
| PVT-Tiny [83] | 13.2 | 1.9 | 75.1 |
| PoolFormer-S12 [94] | 11.9 | 2.0 | 77.2 |
| PVTv2-B1 [82] | 13.1 | 2.1 | 78.7 |
| VAN-Small(Our) | 13.9 | 2.5 | 81.1 |
| ResNet50 [29] | 25.6 | 4.1 | 76.5 |
| ResNeXt50-32x4d [90] | 25.0 | 4.3 | 77.6 |
| RegNetY-4G [61] | 21.0 | 4.0 | 80.0 |
| DeiT-Small/16 [74] | 22.1 | 4.6 | 79.8 |
| T2T-ViT _t -14 [95] | 21.5 | 6.1 | 81.7 |
| PVT-Small [83] | 24.5 | 3.8 | 79.8 |
| TNT-S [26] | 23.8 | 5.2 | 81.3 |
| ResMLP-24 [73] | 30.0 | 6.0 | 79.4 |
| gMLP-S [46] | 20.0 | 4.5 | 79.6 |
| Swin-T [52] | 28.3 | 4.5 | 81.3 |
| PoolFormer-S24 [94] | 21.4 | 3.6 | 80.3 |
| Twins-SVT-S [12] | 24.0 | 2.8 | 81.7 |
| PVTv2-B2 [82] | 25.4 | 4.0 | 82.0 |
| Focal-T [92] | 29.1 | 4.9 | 82.2 |
| ConvNeXt-T [53] | 28.6 | 4.5 | 82.1 |
| VAN-Base(Our) | 26.6 | 5.0 | 82.8 |
| ResNet101 [29] | 44.7 | 7.9 | 77.4 |
| ResNeXt101-32x4d [90] | 44.2 | 8.0 | 78.8 |
| RegNetY-8G [61] | 39.0 | 8.0 | 81.7 |
| Mixer-B/16 | 59.0 | 11.6 | 76.4 |
| T2T-ViT _t -19 [95] | 39.2 | 9.8 | 82.4 |
| PVT-Medium [83] | 44.2 | 6.7 | 81.2 |
| PVT-Large [83] | 61.4 | 9.8 | 81.7 |
| Swin-S [52] | 49.6 | 8.7 | 83.0 |
| ConvNeXt-S [52] | 50.1 | 8.7 | 83.1 |
| PVTv2-B3 [82] | 45.2 | 6.9 | 83.2 |
| Focal-S [92] | 51.1 | 9.1 | 83.5 |
| VAN-Large(Our) | 44.8 | 9.0 | 83.9 |

vs. 75.4%), showing the importance of local structural information in image processing.

- **DW-D-Conv.** DW-D-Conv donates depth-wise dilation convolution which plays a role in capturing long-range dependence in LKA. Without it, the classification performance will drop by 1.3% (74.1% vs. 75.4%) which confirms our viewpoint of long-range dependence is critical for visual tasks.

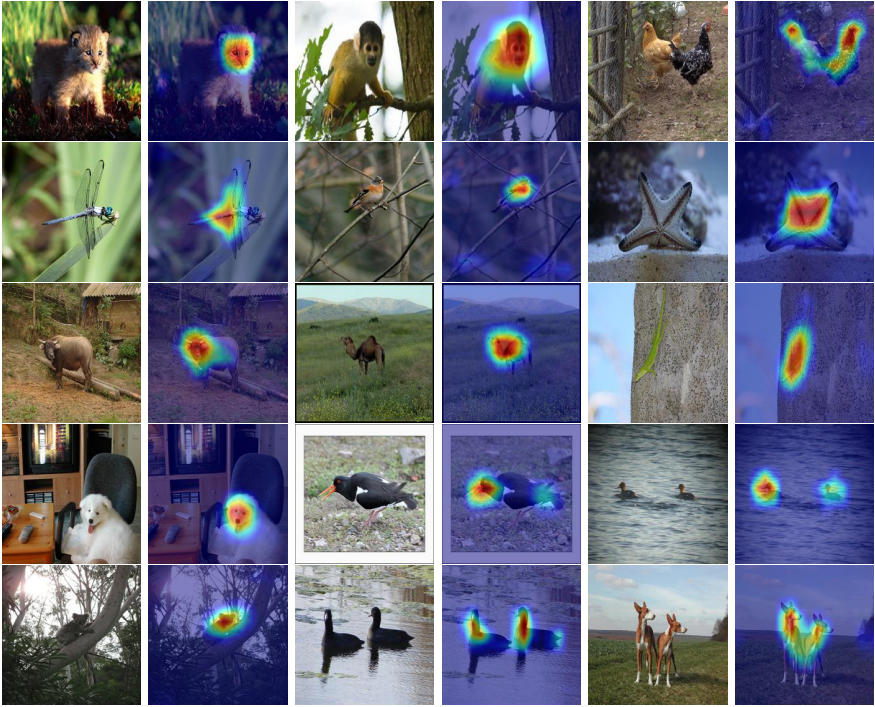


Fig. 4. Visualization results. All images come from different categories in ImageNet validation set. CAM is produced by using VAN-Base model and Grad-CAM [66]. Left: original image, Right: class activation map.

- **Attention Mechanism.** The introduction of the attention mechanism can be regarded as making network achieve adaptive property. Benefited from it, the VAN-Tiny achieves about 1.1% (74.3% vs. 75.4%) improvement.
- 1×1 **Conv.** Here, 1×1 Conv captures relationship in channel dimension. Combining with attention mechanism, it introduces adaptability in channel dimension. It brings about 0.8% (74.1% vs. 75.4%) improvement which proves the necessity of the adaptability in channel dimension.

Through the above analysis, we can find that our proposed LKA can utilize local information, capture long-distance dependencies, and have adaptability in both channel and spatial dimension. Furthermore, experimental results prove all properties are positive for recognition tasks. Although standard convolution can make full use of the local contextual information, it ignores long-range dependencies and adaptability. As for self-attention, although it can capture long-range dependencies and has adaptability in spatial dimensions, it neglects the local information and the adaptability in the channel dimension. Meanwhile, We also summarize above discussion in Tab. 1.

Table 6. Object detection on COCO 2017 dataset. #P means parameter. RetinaNet 1× donates models are based on RetinaNet [44] and we train them for 12 epochs.

| Backbone | RetinaNet 1× | | | | | | |
|---------------------|--------------|-------------|------------------|------------------|-----------------|-----------------|-----------------|
| | #P (M) | AP | AP ₅₀ | AP ₇₅ | AP _S | AP _M | AP _L |
| VAN-Tiny(Our) | 13.4 | 38.8 | 58.8 | 41.3 | 23.4 | 42.8 | 50.9 |
| ResNet18 [29] | 21.3 | 31.8 | 49.6 | 33.6 | 16.3 | 34.3 | 43.2 |
| PoolFormer-S12 [83] | 21.7 | 36.2 | 56.2 | 38.2 | 20.8 | 39.1 | 48.0 |
| PVT-Tiny [83] | 23.0 | 36.7 | 56.9 | 38.9 | 22.6 | 38.8 | 50.0 |
| VAN-Small(Our) | 23.6 | 42.3 | 63.1 | 45.1 | 26.1 | 46.2 | 54.1 |
| ResNet50 [29] | 37.7 | 36.3 | 55.3 | 38.6 | 19.3 | 40.0 | 48.8 |
| PVT-Small [83] | 34.2 | 40.4 | 61.3 | 43.0 | 25.0 | 42.9 | 55.7 |
| PoolFormer-S24 [94] | 31.1 | 38.9 | 59.7 | 41.3 | 23.3 | 42.1 | 51.8 |
| PoolFormer-S36 [94] | 40.6 | 39.5 | 60.5 | 41.8 | 22.5 | 42.9 | 52.4 |
| VAN-Base(Our) | 36.3 | 44.9 | 65.7 | 48.4 | 27.4 | 49.2 | 58.7 |
| ResNet101 [29] | 56.7 | 38.5 | 57.8 | 41.2 | 21.4 | 42.6 | 51.1 |
| PVT-Medium [83] | 53.9 | 41.9 | 63.1 | 44.3 | 25.0 | 44.9 | 57.6 |
| VAN-Large (Our) | 54.5 | 46.1 | 67.0 | 49.7 | 28.4 | 50.1 | 59.8 |

Comparison with Existing Methods. Tab. 5 presents the comparison of VAN with other MLPs, CNNs and ViTs. VAN outperforms common CNNs (ResNet [29], ResNeXt [90], ConvNeXt [53], *etc.*), ViTs (DeiT [74], PVT [83] and Swin-Transformer [52], *etc.*) and MLPs (MLP-Mixer [72], ResMLP [73], gMLP [46], *etc.*) with similar parameters and computational cost. In the following discussion, we will choose a representative network in each category.

ConvNeXt [53] is a special CNN which absorbs the some advantages of ViTs such as large receptive field (7×7 convolution) and advanced training strategy(300 epochs, data augmentation, *etc.*). Compared VAN with ConvNeXt [53], VAN-Base surpasses ConvNeXt-T by 0.7% (82.8% vs. 82.1%) since VAN has larger receptive field and adaptive ability. Swin-Transformer is a well-known ViT variant that adopts local attention and shifted window manner. Due to that VAN is friendly for 2D structural information, has larger receptive field and achieves adaptability in channel dimension, VAN-Base surpasses Swin-T by 1.5% (82.8% vs. 81.3%). As for MLPs, we choose gMLP [46]. VAN-Base surpass gMLP-S [46] by 3.2% (82.8% vs. 79.6%) which reflects the importance of locality.

Visualization Class activation mapping (CAM) is a popular tool to visualize the discriminative regions (attention maps). We adopt Grad-CAM [66] to visualize the attentions on the ImageNet validation set produced by VAN-Base model. Results in Fig. 4 show that VAN-Base can clearly focus on the target objects. Thus, the visualizations intuitively demonstrate the effectiveness of our method.

4.2 Object Detection

Settings. We conduct object detection and instance segmentation experiments on COCO 2017 benchmark [45], which contains 118K images in training

Table 7. Object detection and instance segmentation on COCO 2017 dataset. #P means parameter. Mask R-CNN 1× donates models are based on Mask R-CNN [28] and we train them for 12 epochs. AP^b and AP^m refer to bounding box AP and mask AP respectively.

| Backbone | Mask R-CNN 1× | | | | | | |
|-----------------------|---------------|-----------------|-------------------------------|-------------------------------|-----------------|-------------------------------|-------------------------------|
| | #P (M) | AP ^b | AP ^b ₅₀ | AP ^b ₇₅ | AP ^m | AP ^m ₅₀ | AP ^m ₇₅ |
| VAN-Tiny(Our) | 23.9 | 40.2 | 62.6 | 44.4 | 37.6 | 59.6 | 40.4 |
| ResNet18 [29] | 31.2 | 34.0 | 54.0 | 36.7 | 31.2 | 51.0 | 32.7 |
| PoolFormer-S12 [94] | 31.6 | 37.3 | 59.0 | 40.1 | 34.6 | 55.8 | 36.9 |
| PVT-Tiny [83] | 32.9 | 36.7 | 59.2 | 39.3 | 35.1 | 56.7 | 37.3 |
| VAN-Small(Our) | 33.5 | 42.6 | 64.2 | 46.7 | 38.9 | 61.2 | 41.7 |
| ResNet50 [29] | 44.2 | 38.0 | 58.6 | 41.4 | 34.4 | 55.1 | 36.7 |
| PVT-Small [83] | 44.1 | 40.4 | 62.9 | 43.8 | 37.8 | 60.1 | 40.3 |
| PoolFormer-S24 [94] | 41.0 | 40.1 | 62.2 | 43.4 | 37.0 | 59.1 | 39.6 |
| PoolFormer-S36 [94] | 50.5 | 41.0 | 63.1 | 44.8 | 37.7 | 60.1 | 40.0 |
| VAN-Base(Our) | 46.2 | 46.4 | 67.8 | 51.0 | 41.8 | 65.2 | 44.9 |
| ResNet101 [29] | 63.2 | 40.4 | 61.1 | 44.2 | 36.4 | 57.7 | 38.8 |
| ResNeXt101-32x4d [90] | 62.8 | 41.9 | 62.5 | 45.9 | 37.5 | 59.4 | 40.2 |
| PVT-Medium [83] | 63.9 | 42.0 | 64.4 | 45.6 | 39.0 | 61.6 | 42.1 |
| VAN-Large (Our) | 64.4 | 47.1 | 67.9 | 51.9 | 42.2 | 65.4 | 45.5 |

Table 8. lznComparison with the state-of-the-art vision backbones on COCO 2017 benchmark. All models are trained for 36 epochs. We calculate FLOPs with input size of 1,280 × 800.

| Backbone | Method | AP ^b | AP ^b ₅₀ | AP ^b ₇₅ | #P (M) | GFLOPs |
|-----------------|---------------------------|-----------------|-------------------------------|-------------------------------|--------|--------|
| Swin-T [29] | Mask R-CNN [28] | 46.0 | 68.1 | 50.3 | 48 | 264 |
| ConvNeXt-T [52] | | 46.2 | 67.9 | 50.8 | 48 | 262 |
| VAN-Base(Our) | | 47.4 | 68.6 | 51.6 | 46 | 273 |
| ResNet50 [29] | Cascade Mask R-CNN [6] | 46.3 | 64.3 | 50.5 | 82 | 739 |
| Swin-T [52] | | 50.5 | 69.3 | 54.9 | 86 | 745 |
| ConvNeXt-T [53] | | 50.4 | 69.1 | 54.8 | 86 | 741 |
| VAN-Base(Our) | | 50.5 | 69.3 | 54.6 | 84 | 752 |
| ResNet50 [29] | ATSS [101] | 43.5 | 61.9 | 47.0 | 32 | 205 |
| Swin-T [52] | | 47.2 | 66.5 | 51.3 | 36 | 215 |
| VAN-Base(Our) | | 49.1 | 68.2 | 53.3 | 34 | 221 |
| ResNet50 [29] | GFL [42] | 44.5 | 63.0 | 48.3 | 32 | 208 |
| Swin-T [52] | | 47.6 | 66.8 | 51.7 | 36 | 215 |
| VAN-Base(Our) | | 49.3 | 68.5 | 53.5 | 34 | 224 |
| ResNet50 [29] | Sparse R-CNN [70] | 44.5 | 63.4 | 48.2 | 106 | 166 |
| Swin-T [52] | | 47.9 | 67.3 | 52.3 | 110 | 172 |
| VAN-Base(Our) | | 49.1 | 68.9 | 53.6 | 108 | 178 |

set and 5K images in validation set. MMDetection [8] is used as the codebase to implement detection models. For fair comparison, we adopt the same training/validating strategies with Swin Transformer [52] and PoolFormer [94]. Many kinds of detection models (*e.g.*, Mask R-CNN [28], RetinaNet [44], Cascade Mask

Table 9. Results of semantic segmentation on ADE20K [105] validation set. The upper and lower part are obtained under two different training/validation schemes following [94] and [52].

| Method | Backbone | #Param (M) | GFLOPs | mIoU (%) |
|-------------------|-----------------------|------------|-------------|-------------|
| Semantic FPN [38] | PVTv2-B0 [82] | 8 | 25 | 37.2 |
| | VAN-Tiny | 8 | 26 | 38.5 |
| | ResNet18 [29] | 16 | 32 | 32.9 |
| | PVT-Tiny [83] | 17 | 33 | 35.7 |
| | PoolFormer-S12 [94] | 16 | 31 | 37.2 |
| | PVTv2-B1 [82] | 18 | 34 | 42.5 |
| | VAN-Small | 18 | 35 | 42.9 |
| | ResNet50 [29] | 29 | 46 | 36.7 |
| | PVT-Small [83] | 28 | 45 | 39.8 |
| | PoolFormer-S24 [94] | 23 | 39 | 40.3 |
| | PVTv2-B2 [82] | 29 | 46 | 45.2 |
| | VAN-Base | 30 | 48 | 46.7 |
| | ResNet101 [29] | 48 | 65 | 38.8 |
| | ResNeXt101-32x4d [90] | 47 | 65 | 39.7 |
| | PVT-Medium [83] | 48 | 61 | 43.5 |
| | PoolFormer-S36 [94] | 35 | 48 | 42.0 |
| PVTv2-B3 [82] | 49 | 62 | 47.3 | |
| VAN-Large | 49 | 68 | 48.1 | |
| DANet [18] | ResNet-101 [29] | 69 | 1119 | 45.2 |
| DLab.v3+ [10] | | 63 | 1021 | 44.1 |
| OCRNet [96] | | 56 | 923 | 45.3 |
| UperNet [88] | | 86 | 1029 | 44.9 |
| UperNet [88] | Swin-T [52] | 60 | 945 | 46.1 |
| | Swin-S [52] | 81 | 1038 | 49.3 |
| | VAN-Tiny | 32 | 214 | 41.1 |
| | VAN-Small | 44 | 224 | 44.9 |
| | VAN-Base | 57 | 237 | 48.3 |
| | VAN-Large | 75 | 258 | 50.1 |

R-CNN [6], Sparse R-CNN [70], *etc.*) are included to demonstrate the effectiveness of our method. All backbone models are pre-trained on ImageNet training set.

Results. According to Tab. 6 and Tab. 7, we find that VAN surpasses CNN-based method ResNet [29] and transformer-based method PVT [83] with a large margin under RetinaNet [44] 1x and Mask R-CNN [28] 1x settings. Besides, we also compare the state-of-the-art methods Swin transformer [52] and ConvNeXt [53] in Tab. 8. Results show that VAN achieves the state-of-the-art performance with different detection methods such as Mask R-CNN [28] and Sparse R-CNN [70].

4.3 Semantic Segmentation

Settings. We conduct experiments on ADE20K [105], which contains 150 semantic categories for semantic segmentation. It consists of 20,000, 2,000 and 3,000 separately for training, validation and testing. MMSEG [13] is used as the base framework and two famous segmentation heads, Semantic FPN [38] and UperNet [88], are employed for evaluating our VAN backbones. For a fair comparison, we adopt two training/validating schemes following [94] and [52] and quantitative results on the validation set are shown in the upper and lower part in Tab. 9, respectively. All backbone models are pre-trained on ImageNet training set.

Results. From the upper part in Tab. 9, compared with different backbones using FPN [38], VAN-based methods are superior to CNN-based (ResNet [29], ResNeXt [90]) or transformer-based (PVT [83], PoolFormer [94], PVTv2 [82]) methods. For instance, we surpass four PVTv2 [82] variants by +1.3 (tiny), +0.4 (small), +1.5 (base), +0.8 (large) mIoU under comparable parameters and FLOPs. In the lower part in Tab. 9, when compared with previous state-of-the-art CNN-based methods and Swin-Transformer based methods, four VAN variants also show excellent performance with smaller parameters and FLOPs. For instance, based on UperNet [88], VAN-Base is +3.4 and +2.2 mIoU higher than ResNet-101 and Swin-T, respectively.

5 Future Work

In the future, we will continue perfecting VAN in followings directions:

- **Continuous improvement of the structure itself.** In this paper, we only demonstrate an intuitive structure. There are a lot of potential improvements such as adopting larger kernel, introducing multi-scale structure [19] and using multi-branch structure [71].
- **Large-scale self-supervised learning and transfer learning.** VAN naturally combines the advantages of CNNs and ViTs. On the one hand, VAN can make use of the 2D structure information of images. On the other hand, VAN can dynamically adjust the output according to the input image which is suit for self-supervised learning and transfer learning [4,27]. Combining the above two points, we believe VAN can achieve better performance in image self-supervised learning and transfer learning field.
- **More application areas.** Due to the limited resource, we only show excellent performance in visual tasks. Whether VANs can perform well in other areas like TCN [3] in NLP is still worth exploring. we look forward to seeing VANs showing excellent performance in different areas and becoming a general model.

6 Conclusion

In this paper, we present a novel visual attention LKA which combines the advantages of convolution and self-attention. Based on LKA, we build a vision backbone VAN that achieves the state-of-the-art performance in some visual tasks, including image classification, object detection, semantic segmentation, *etc.* In the future, we will continue to improve this framework from the directions mentioned in Sec. 5.

7 Acknowledgement

This work was supported by the National Key R&D Program(), the Natural Science Foundation of China (Project 61521002, 61922046), and Tsinghua-Tencent Joint Laboratory for Internet Innovation Technology.

References

1. Ali, A., Touvron, H., Caron, M., Bojanowski, P., Douze, M., Joulin, A., Laptev, I., Neverova, N., Synnaeve, G., Verbeek, J., et al.: Xcit: Cross-covariance image transformers. *Advances in neural information processing systems* **34** (2021)
2. Ba, J.L., Kiros, J.R., Hinton, G.E.: Layer normalization (2016)
3. Bai, S., Kolter, J.Z., Koltun, V.: An empirical evaluation of generic convolutional and recurrent networks for sequence modeling. *arXiv preprint arXiv:1803.01271* (2018)
4. Bao, H., Dong, L., Piao, S., Wei, F.: BEit: BERT pre-training of image transformers. In: *International Conference on Learning Representations* (2022)
5. Brown, T., Mann, B., Ryder, N., Subbiah, M., Kaplan, J.D., Dhariwal, P., Nee-lakantan, A., Shyam, P., Sastry, G., Askell, A., et al.: Language models are few-shot learners. *Advances in neural information processing systems* **33**, 1877–1901 (2020)
6. Cai, Z., Vasconcelos, N.: Cascade r-cnn: High quality object detection and instance segmentation. *IEEE Transactions on Pattern Analysis and Machine Intelligence* (2019)
7. Carion, N., Massa, F., Synnaeve, G., Usunier, N., Kirillov, A., Zagoruyko, S.: End-to-end object detection with transformers. In: *European Conference on Computer Vision*. pp. 213–229. Springer (2020)
8. Chen, K., Wang, J., Pang, J., Cao, Y., Xiong, Y., Li, X., Sun, S., Feng, W., Liu, Z., Xu, J., et al.: Mmdetection: Open mmlab detection toolbox and benchmark. *arXiv preprint arXiv:1906.07155* (2019)
9. Chen, L.C., Papandreou, G., Kokkinos, I., Murphy, K., Yuille, A.L.: Semantic image segmentation with deep convolutional nets and fully connected crfs. *arXiv preprint arXiv:1412.7062* (2014)
10. Chen, L.C., Zhu, Y., Papandreou, G., Schroff, F., Adam, H.: Encoder-decoder with atrous separable convolution for semantic image segmentation. In: *Proceedings of the European conference on computer vision (ECCV)*. pp. 801–818 (2018)
11. Chen, L., Zhang, H., Xiao, J., Nie, L., Shao, J., Liu, W., Chua, T.S.: Sca-cnn: Spatial and channel-wise attention in convolutional networks for image captioning. In: *Proceedings of the IEEE conference on computer vision and pattern recognition*. pp. 5659–5667 (2017)
12. Chu, X., Tian, Z., Wang, Y., Zhang, B., Ren, H., Wei, X., Xia, H., Shen, C.: Twins: Revisiting the design of spatial attention in vision transformers. *Advances in Neural Information Processing Systems* **34** (2021)
13. Contributors, M.: MMSegmentation: Openmmlab semantic segmentation toolbox and benchmark. <https://github.com/open-mmlab/mms Segmentation> (2020)
14. Dai, J., Qi, H., Xiong, Y., Li, Y., Zhang, G., Hu, H., Wei, Y.: Deformable convolutional networks. In: *Proceedings of the IEEE international conference on computer vision*. pp. 764–773 (2017)
15. Deng, J., Dong, W., Socher, R., Li, L.J., Li, K., Fei-Fei, L.: Imagenet: A large-scale hierarchical image database. In: *2009 IEEE conference on computer vision and pattern recognition*. pp. 248–255. Ieee (2009)
16. Devlin, J., Chang, M.W., Lee, K., Toutanova, K.: Bert: Pre-training of deep bidirectional transformers for language understanding. *arXiv preprint arXiv:1810.04805* (2018)
17. Dosovitskiy, A., Beyer, L., Kolesnikov, A., Weissenborn, D., Zhai, X., Unterthiner, T., Dehghani, M., Minderer, M., Heigold, G., Gelly, S., et al.: An image is worth

- 16x16 words: Transformers for image recognition at scale. In: Int. Conf. Learn. Represent. (2020)
18. Fu, J., Liu, J., Tian, H., Li, Y., Bao, Y., Fang, Z., Lu, H.: Dual attention network for scene segmentation. In: Proceedings of the IEEE/CVF Conference on Computer Vision and Pattern Recognition. pp. 3146–3154 (2019)
 19. Gao, S., Cheng, M.M., Zhao, K., Zhang, X.Y., Yang, M.H., Torr, P.H.: Res2net: A new multi-scale backbone architecture. *IEEE transactions on pattern analysis and machine intelligence* (2019)
 20. Geng, Z., Guo, M.H., Chen, H., Li, X., Wei, K., Lin, Z.: Is attention better than matrix decomposition? In: International Conference on Learning Representations (2021)
 21. Gottlieb, J.P., Kusunoki, M., Goldberg, M.E.: The representation of visual salience in monkey parietal cortex. *Nature* **391**(6666), 481–484 (1998)
 22. Guo, M.H., Cai, J.X., Liu, Z.N., Mu, T.J., Martin, R.R., Hu, S.M.: Pct: Point cloud transformer. *Computational Visual Media* **7**(2), 187–199 (2021)
 23. Guo, M.H., Liu, Z.N., Mu, T.J., Hu, S.M.: Beyond self-attention: External attention using two linear layers for visual tasks. *arXiv preprint arXiv:2105.02358* (2021)
 24. Guo, M.H., Liu, Z.N., Mu, T.J., Liang, D., Martin, R.R., Hu, S.M.: Can attention enable mlps to catch up with cnns? *Computational Visual Media* **7**(3), 283–288 (2021)
 25. Guo, M.H., Xu, T.X., Liu, J.J., Liu, Z.N., Jiang, P.T., Mu, T.J., Zhang, S.H., Martin, R.R., Cheng, M.M., Hu, S.M.: Attention mechanisms in computer vision: A survey (2021)
 26. Han, K., Xiao, A., Wu, E., Guo, J., Xu, C., Wang, Y.: Transformer in transformer. *Advances in Neural Information Processing Systems* **34** (2021)
 27. He, K., Chen, X., Xie, S., Li, Y., Dollár, P., Girshick, R.: Masked autoencoders are scalable vision learners (2021)
 28. He, K., Gkioxari, G., Dollar, P., Girshick, R.: Mask r-cnn. In: Proceedings of the IEEE International Conference on Computer Vision (ICCV) (Oct 2017)
 29. He, K., Zhang, X., Ren, S., Sun, J.: Deep residual learning for image recognition. In: Proceedings of the IEEE conference on computer vision and pattern recognition. pp. 770–778 (2016)
 30. Hendrycks, D., Gimpel, K.: Gaussian error linear units (gelus) (2020)
 31. Howard, A.G., Zhu, M., Chen, B., Kalenichenko, D., Wang, W., Weyand, T., Andreetto, M., Adam, H.: Mobilenets: Efficient convolutional neural networks for mobile vision applications. *arXiv preprint arXiv:1704.04861* (2017)
 32. Hu, H., Gu, J., Zhang, Z., Dai, J., Wei, Y.: Relation networks for object detection. In: Proceedings of the IEEE conference on computer vision and pattern recognition. pp. 3588–3597 (2018)
 33. Hu, J., Shen, L., Albanie, S., Sun, G., Vedaldi, A.: Gather-excite: Exploiting feature context in convolutional neural networks. *Advances in neural information processing systems* **31** (2018)
 34. Hu, J., Shen, L., Sun, G.: Squeeze-and-excitation networks. In: Proceedings of the IEEE conference on computer vision and pattern recognition. pp. 7132–7141 (2018)
 35. Huang, G., Liu, Z., Van Der Maaten, L., Weinberger, K.Q.: Densely connected convolutional networks. In: Proceedings of the IEEE conference on computer vision and pattern recognition. pp. 4700–4708 (2017)

36. Ioffe, S., Szegedy, C.: Batch normalization: Accelerating deep network training by reducing internal covariate shift. In: International conference on machine learning. pp. 448–456. PMLR (2015)
37. Kingma, D.P., Ba, J.: Adam: A method for stochastic optimization (2017)
38. Kirillov, A., Girshick, R., He, K., Dollár, P.: Panoptic feature pyramid networks. In: Proceedings of the IEEE/CVF Conference on Computer Vision and Pattern Recognition. pp. 6399–6408 (2019)
39. Krizhevsky, A., Sutskever, I., Hinton, G.E.: Imagenet classification with deep convolutional neural networks. *Advances in neural information processing systems* **25**, 1097–1105 (2012)
40. LeCun, Y., Boser, B., Denker, J.S., Henderson, D., Howard, R.E., Hubbard, W., Jackel, L.D.: Backpropagation applied to handwritten zip code recognition. *Neural computation* **1**(4), 541–551 (1989)
41. LeCun, Y., Bottou, L., Bengio, Y., Haffner, P.: Gradient-based learning applied to document recognition. *Proceedings of the IEEE* **86**(11), 2278–2324 (1998)
42. Li, X., Wang, W., Wu, L., Chen, S., Hu, X., Li, J., Tang, J., Yang, J.: Generalized focal loss: Learning qualified and distributed bounding boxes for dense object detection. *Advances in Neural Information Processing Systems* **33**, 21002–21012 (2020)
43. Lin, M., Chen, Q., Yan, S.: Network in network. In: ICLR (2014)
44. Lin, T.Y., Goyal, P., Girshick, R., He, K., Dollár, P.: Focal loss for dense object detection. In: Proceedings of the IEEE international conference on computer vision. pp. 2980–2988 (2017)
45. Lin, T.Y., Maire, M., Belongie, S., Hays, J., Perona, P., Ramanan, D., Dollár, P., Zitnick, C.L.: Microsoft coco: Common objects in context. In: European conference on computer vision. pp. 740–755. Springer (2014)
46. Liu, H., Dai, Z., So, D., Le, Q.V.: Pay attention to MLPs. In: Beygelzimer, A., Dauphin, Y., Liang, P., Vaughan, J.W. (eds.) *Advances in Neural Information Processing Systems* (2021)
47. Liu, R., Deng, H., Huang, Y., Shi, X., Lu, L., Sun, W., Wang, X., Dai, J., Li, H.: Decoupled spatial-temporal transformer for video inpainting. *arXiv preprint arXiv:2104.06637* (2021)
48. Liu, R., Deng, H., Huang, Y., Shi, X., Lu, L., Sun, W., Wang, X., Dai, J., Li, H.: Fuseformer: Fusing fine-grained information in transformers for video inpainting. In: Proceedings of the IEEE/CVF International Conference on Computer Vision. pp. 14040–14049 (2021)
49. Liu, R., Li, Y., Tao, L., Liang, D., Hu, S.M., Zheng, H.T.: Are we ready for a new paradigm shift? a survey on visual deep mlp (2021)
50. Liu, S., Li, F., Zhang, H., Yang, X., Qi, X., Su, H., Zhu, J., Zhang, L.: DAB-DETR: Dynamic anchor boxes are better queries for DETR. In: International Conference on Learning Representations (2022)
51. Liu, S., Zhang, L., Yang, X., Su, H., Zhu, J.: Query2label: A simple transformer way to multi-label classification (2021)
52. Liu, Z., Lin, Y., Cao, Y., Hu, H., Wei, Y., Zhang, Z., Lin, S., Guo, B.: Swin transformer: Hierarchical vision transformer using shifted windows. In: *Int. Conf. Comput. Vis.* (2021)
53. Liu, Z., Mao, H., Wu, C.Y., Feichtenhofer, C., Darrell, T., Xie, S.: A convnet for the 2020s (2022)
54. Loshchilov, I., Hutter, F.: Sgdr: Stochastic gradient descent with warm restarts. *arXiv preprint arXiv:1608.03983* (2016)

55. Loshchilov, I., Hutter, F.: Decoupled weight decay regularization (2019)
56. Mnih, V., Heess, N., Graves, A., et al.: Recurrent models of visual attention. In: *Advances in neural information processing systems*. pp. 2204–2212 (2014)
57. Müller, R., Kornblith, S., Hinton, G.E.: When does label smoothing help? *Advances in neural information processing systems* **32** (2019)
58. Park, J., Woo, S., Lee, J.Y., Kweon, I.S.: Bam: Bottleneck attention module. arXiv preprint arXiv:1807.06514 (2018)
59. Polyak, B.T., Juditsky, A.B.: Acceleration of stochastic approximation by averaging. *SIAM journal on control and optimization* **30**(4), 838–855 (1992)
60. Qin, Z., Zhang, P., Wu, F., Li, X.: Fcanet: Frequency channel attention networks. In: *Proceedings of the IEEE/CVF International Conference on Computer Vision*. pp. 783–792 (2021)
61. Radosavovic, I., Kosaraju, R.P., Girshick, R., He, K., Dollár, P.: Designing network design spaces. In: *Proceedings of the IEEE/CVF Conference on Computer Vision and Pattern Recognition*. pp. 10428–10436 (2020)
62. Ramachandran, P., Parmar, N., Vaswani, A., Bello, I., Levskaya, A., Shlens, J.: Stand-alone self-attention in vision models. arXiv preprint arXiv:1906.05909 (2019)
63. Rosenblatt, F.: The perceptron: a probabilistic model for information storage and organization in the brain. *Psychological review* **65**(6), 386 (1958)
64. Rumelhart, D.E., Hinton, G.E., Williams, R.J.: Learning internal representations by error propagation. Tech. rep., California Univ San Diego La Jolla Inst for Cognitive Science (1985)
65. Sandler, M., Howard, A., Zhu, M., Zhmoginov, A., Chen, L.C.: Mobilenetv2: Inverted residuals and linear bottlenecks. In: *Proceedings of the IEEE conference on computer vision and pattern recognition*. pp. 4510–4520 (2018)
66. Selvaraju, R.R., Cogswell, M., Das, A., Vedantam, R., Parikh, D., Batra, D.: Grad-cam: Visual explanations from deep networks via gradient-based localization. In: *Proceedings of the IEEE international conference on computer vision*. pp. 618–626 (2017)
67. Sermanet, P., Eigen, D., Zhang, X., Mathieu, M., Fergus, R., LeCun, Y.: Overfeat: Integrated recognition, localization and detection using convolutional networks. arXiv preprint arXiv:1312.6229 (2013)
68. Simonyan, K., Zisserman, A.: Very deep convolutional networks for large-scale image recognition. arXiv preprint arXiv:1409.1556 (2014)
69. Srinivas, A., Lin, T.Y., Parmar, N., Shlens, J., Abbeel, P., Vaswani, A.: Bottleneck transformers for visual recognition. In: *Proceedings of the IEEE/CVF Conference on Computer Vision and Pattern Recognition*. pp. 16519–16529 (2021)
70. Sun, P., Zhang, R., Jiang, Y., Kong, T., Xu, C., Zhan, W., Tomizuka, M., Li, L., Yuan, Z., Wang, C., et al.: Sparse r-cnn: End-to-end object detection with learnable proposals. In: *Proceedings of the IEEE/CVF Conference on Computer Vision and Pattern Recognition*. pp. 14454–14463 (2021)
71. Szegedy, C., Liu, W., Jia, Y., Sermanet, P., Reed, S., Anguelov, D., Erhan, D., Vanhoucke, V., Rabinovich, A.: Going deeper with convolutions. In: *Proceedings of the IEEE conference on computer vision and pattern recognition*. pp. 1–9 (2015)
72. Tolstikhin, I.O., Houlsby, N., Kolesnikov, A., Beyer, L., Zhai, X., Unterthiner, T., Yung, J., Steiner, A., Keysers, D., Uszkoreit, J., et al.: Mlp-mixer: An all-mlp architecture for vision. *Advances in Neural Information Processing Systems* **34** (2021)

73. Touvron, H., Bojanowski, P., Caron, M., Cord, M., El-Nouby, A., Grave, E., Izacard, G., Joulin, A., Synnaeve, G., Verbeek, J., et al.: Resmlp: Feedforward networks for image classification with data-efficient training. arXiv preprint arXiv:2105.03404 (2021)
74. Touvron, H., Cord, M., Douze, M., Massa, F., Sablayrolles, A., Jégou, H.: Training data-efficient image transformers & distillation through attention. In: International Conference on Machine Learning. pp. 10347–10357. PMLR (2021)
75. Touvron, H., Cord, M., Sablayrolles, A., Synnaeve, G., Jégou, H.: Going deeper with image transformers. In: Proceedings of the IEEE/CVF International Conference on Computer Vision. pp. 32–42 (2021)
76. Treisman, A.M., Gelade, G.: A feature-integration theory of attention. *Cognitive psychology* **12**(1), 97–136 (1980)
77. Tsotsos, J.K., Culhane, S.M., Wai, W.Y.K., Lai, Y., Davis, N., Nuflo, F.: Modeling visual attention via selective tuning. *Artificial intelligence* **78**(1-2), 507–545 (1995)
78. Vaswani, A., Shazeer, N., Parmar, N., Uszkoreit, J., Jones, L., Gomez, A.N., Kaiser, Ł., Polosukhin, I.: Attention is all you need. In: Advances in neural information processing systems. pp. 5998–6008 (2017)
79. Wang, F., Jiang, M., Qian, C., Yang, S., Li, C., Zhang, H., Wang, X., Tang, X.: Residual attention network for image classification. In: Proceedings of the IEEE conference on computer vision and pattern recognition. pp. 3156–3164 (2017)
80. Wang, J., Sun, K., Cheng, T., Jiang, B., Deng, C., Zhao, Y., Liu, D., Mu, Y., Tan, M., Wang, X., et al.: Deep high-resolution representation learning for visual recognition. *IEEE transactions on pattern analysis and machine intelligence* (2020)
81. Wang, Q., Wu, B., Zhu, P., Li, P., Zuo, W., Hu, Q.: Eca-net: Efficient channel attention for deep convolutional neural networks (2020)
82. Wang, W., Xie, E., Li, X., Fan, D.P., Song, K., Liang, D., Lu, T., Luo, P., Shao, L.: Pvtv2: Improved baselines with pyramid vision transformer. arXiv preprint arXiv:2106.13797 (2021)
83. Wang, W., Xie, E., Li, X., Fan, D.P., Song, K., Liang, D., Lu, T., Luo, P., Shao, L.: Pyramid vision transformer: A versatile backbone for dense prediction without convolutions. In: IEEE ICCV (2021)
84. Wang, X., Girshick, R., Gupta, A., He, K.: Non-local neural networks. In: Proceedings of the IEEE conference on computer vision and pattern recognition. pp. 7794–7803 (2018)
85. Wolfe, J.M., Horowitz, T.S.: What attributes guide the deployment of visual attention and how do they do it? *Nature reviews neuroscience* **5**(6), 495–501 (2004)
86. Woo, S., Park, J., Lee, J.Y., Kweon, I.S.: Cbam: Convolutional block attention module. In: Proceedings of the European conference on computer vision (ECCV). pp. 3–19 (2018)
87. Wu, H., Xiao, B., Codella, N., Liu, M., Dai, X., Yuan, L., Zhang, L.: Cvt: Introducing convolutions to vision transformers. In: Proceedings of the IEEE/CVF International Conference on Computer Vision. pp. 22–31 (2021)
88. Xiao, T., Liu, Y., Zhou, B., Jiang, Y., Sun, J.: Unified perceptual parsing for scene understanding. In: Proceedings of the European Conference on Computer Vision (ECCV). pp. 418–434 (2018)
89. Xie, E., Wang, W., Yu, Z., Anandkumar, A., Alvarez, J.M., Luo, P.: Segformer: Simple and efficient design for semantic segmentation with transformers. *Advances in Neural Information Processing Systems* **34** (2021)

90. Xie, S., Girshick, R., Dollár, P., Tu, Z., He, K.: Aggregated residual transformations for deep neural networks. In: Proceedings of the IEEE conference on computer vision and pattern recognition. pp. 1492–1500 (2017)
91. Xie, S., Liu, S., Chen, Z., Tu, Z.: Attentional shapecontextnet for point cloud recognition. In: Proceedings of the IEEE Conference on Computer Vision and Pattern Recognition. pp. 4606–4615 (2018)
92. Yang, J., Li, C., Zhang, P., Dai, X., Xiao, B., Yuan, L., Gao, J.: Focal self-attention for local-global interactions in vision transformers (2021)
93. Yu, F., Koltun, V.: Multi-scale context aggregation by dilated convolutions. arXiv preprint arXiv:1511.07122 (2015)
94. Yu, W., Luo, M., Zhou, P., Si, C., Zhou, Y., Wang, X., Feng, J., Yan, S.: Metaformer is actually what you need for vision. arXiv preprint arXiv:2111.11418 (2021)
95. Yuan, L., Chen, Y., Wang, T., Yu, W., Shi, Y., Jiang, Z.H., Tay, F.E., Feng, J., Yan, S.: Tokens-to-token vit: Training vision transformers from scratch on imagenet. In: Proceedings of the IEEE/CVF International Conference on Computer Vision (ICCV). pp. 558–567 (October 2021)
96. Yuan, Y., Chen, X., Wang, J.: Object-contextual representations for semantic segmentation. In: Computer Vision–ECCV 2020: 16th European Conference, Glasgow, UK, August 23–28, 2020, Proceedings, Part VI 16. pp. 173–190. Springer (2020)
97. Yuan, Y., Huang, L., Guo, J., Zhang, C., Chen, X., Wang, J.: Ocnet: Object context network for scene parsing. arXiv preprint arXiv:1809.00916 (2018)
98. Yun, S., Han, D., Oh, S.J., Chun, S., Choe, J., Yoo, Y.: Cutmix: Regularization strategy to train strong classifiers with localizable features. In: Proceedings of the IEEE/CVF International Conference on Computer Vision. pp. 6023–6032 (2019)
99. Zhang, H., Goodfellow, I., Metaxas, D., Odena, A.: Self-attention generative adversarial networks. In: International conference on machine learning. pp. 7354–7363. PMLR (2019)
100. Zhang, H., Cisse, M., Dauphin, Y.N., Lopez-Paz, D.: mixup: Beyond empirical risk minimization. arXiv preprint arXiv:1710.09412 (2017)
101. Zhang, S., Chi, C., Yao, Y., Lei, Z., Li, S.Z.: Bridging the gap between anchor-based and anchor-free detection via adaptive training sample selection. In: Proceedings of the IEEE/CVF conference on computer vision and pattern recognition. pp. 9759–9768 (2020)
102. Zhang, X., Zhou, X., Lin, M., Sun, J.: Shufflenet: An extremely efficient convolutional neural network for mobile devices. In: Proceedings of the IEEE conference on computer vision and pattern recognition. pp. 6848–6856 (2018)
103. Zhong, Z., Zheng, L., Kang, G., Li, S., Yang, Y.: Random erasing data augmentation. In: Proceedings of the AAAI Conference on Artificial Intelligence. pp. 13001–13008 (2020)
104. Zhou, B., Khosla, A., Lapedriza, A., Oliva, A., Torralba, A.: Learning deep features for discriminative localization. In: Proceedings of the IEEE conference on computer vision and pattern recognition. pp. 2921–2929 (2016)
105. Zhou, B., Zhao, H., Puig, X., Xiao, T., Fidler, S., Barriuso, A., Torralba, A.: Semantic understanding of scenes through the ade20k dataset. *International Journal of Computer Vision* **127**(3), 302–321 (2019)